DOI: 10.1002/ejoc.200901133

Physicochemical Studies of New Anthocyano-Ellagitannin Hybrid Pigments: About the Origin of the Influence of Oak *C*-Glycosidic Ellagitannins on Wine Color

Stefan Chassaing,[a,b] Dorothée Lefeuvre,[a,b,c] Rémi Jacquet,[a,b] Michael Jourdes,[a,b,c] Laurent Ducasse,[b] Stéphanie Galland,[d] Axelle Grelard,[a] Cédric Saucier,[c] Pierre-Louis Teissedre,[c] Olivier Dangles,*[d] and Stéphane Quideau*[a,b]

Dedicated to Prof. Raymond Brouillard on the occasion of his retirement

Keywords: Natural products / Dyes/Pigments / Anthocyanins / Polyphenols / Ellagitannins

Kinetic and thermodynamic UV/Vis and structural NMR spectroscopic investigations on the anthocyano-ellagitannin hybrid 1-deoxyvescalagin-(1β→8)-oenin revealed that its enhanced color stability relative to that of the red-colored pigment oenin and resulting bathochromism can be rationalized in terms of an intramolecular π-stacking between the grape-derived oenin chromophore and the oak-derived vescalagin 4,6-hexahydroxydiphenoyl moiety. The results led us to suggest that this bathochromism-inducing molecular association could be the first ellagitannin-based molecular-level explanation of the red-to-purple color change that takes place during the aging of wine in oak barrels.

Introduction

Anthocyanins are plant pigments widely found in flowers and fruits, the pigmentation of which varies from red to blue depending on various factors, such as pH, complexation with metal ions, π-stacking interactions with colorless aromatic compounds (i.e., copigmentation), as well as the structure of the anthocyanins themselves.[1] The bright red color of young wines is the result of the release of anthocyanins from red grape skins during the maceration stage of the wine-making process. These native grape pigments, in particular oenin (**1**), the major anthocyanin in *Vitis vinifera* species, progressively disappear during wine maturation as a result of various chemical reactions that slowly lead to more stable wine-specific pigments.[2,3] Several chemical reactions involving other compounds found in wine, such as (oligo)flavanols (i.e., from flavan-3-ols to proanthocyanidins),[4] acetaldehyde,[5] pyruvic acid,[6] or vinylphenols,[7] have been shown to form compounds exhibiting either bluer or more orangey tints (Scheme 1).

Few investigations have taken into account the influence of the container on the modulation of wine color. The faster disappearance of grape anthocyanins in wines aged in oak-made casks compared with those aged in hermetic cement/inox vats has generally been attributed to wood porosity favoring oxidation.[8] However, enabling dioxygen (O_2) diffusion is far from being the only contribution of oak wood to the wine chemical profile, as evidenced for example by the acceleration of the color evolution upon the simple addition of oak chips.[9] Indeed, an aqueous alcoholic solution like wine not only extracts carbohydrate-, lignin-, and fatty acid-derived fragments from toasted oak barrels or chips, but also hydrolyzable tannins.[10] Among the latter figure *C*-glycosidic ellagitannins such as vescalagin (**3**),[11] which is involved in stereoselective condensation reactions with wine nucleophiles, including grape anthocyanins.[12] We wish to report herein our results on the physicochemical characterization of the novel pigments **4** and **5** generated from **3** and the anthocyanin oenin (**1**), as well as from its aglycone malvidin (**2**; Scheme 2).

[a] Institut Européen de Chimie et Biologie,
2 rue Robert Escarpit, 33607 Pessac Cedex, France
E-mail: s.quideau@iecb.u-bordeaux.fr
[b] Institut des Sciences Moléculaires (UMR-CNRS 5255), Université de Bordeaux,
351 cours de la Libération, 33405 Talence Cedex, France
[c] Institut des Sciences de la Vigne et du Vin, Bordeaux-Aquitaine (UMR-INRA 1219), Université de Bordeaux,
210 Chemin de Leysotte CS 50008, 33882 Villenave d'Ornon, France
[d] Université d'Avignon et des Pays de Vaucluse, INRA, UMR 408, 84000 Avignon, France
E-mail: olivier.dangles@univ-avignon.fr
Supporting information for this article is available on the WWW under http://dx.doi.org/10.1002/ejoc.200901133.

 © 2010 Wiley-VCH Verlag GmbH & Co. KGaA, Weinheim

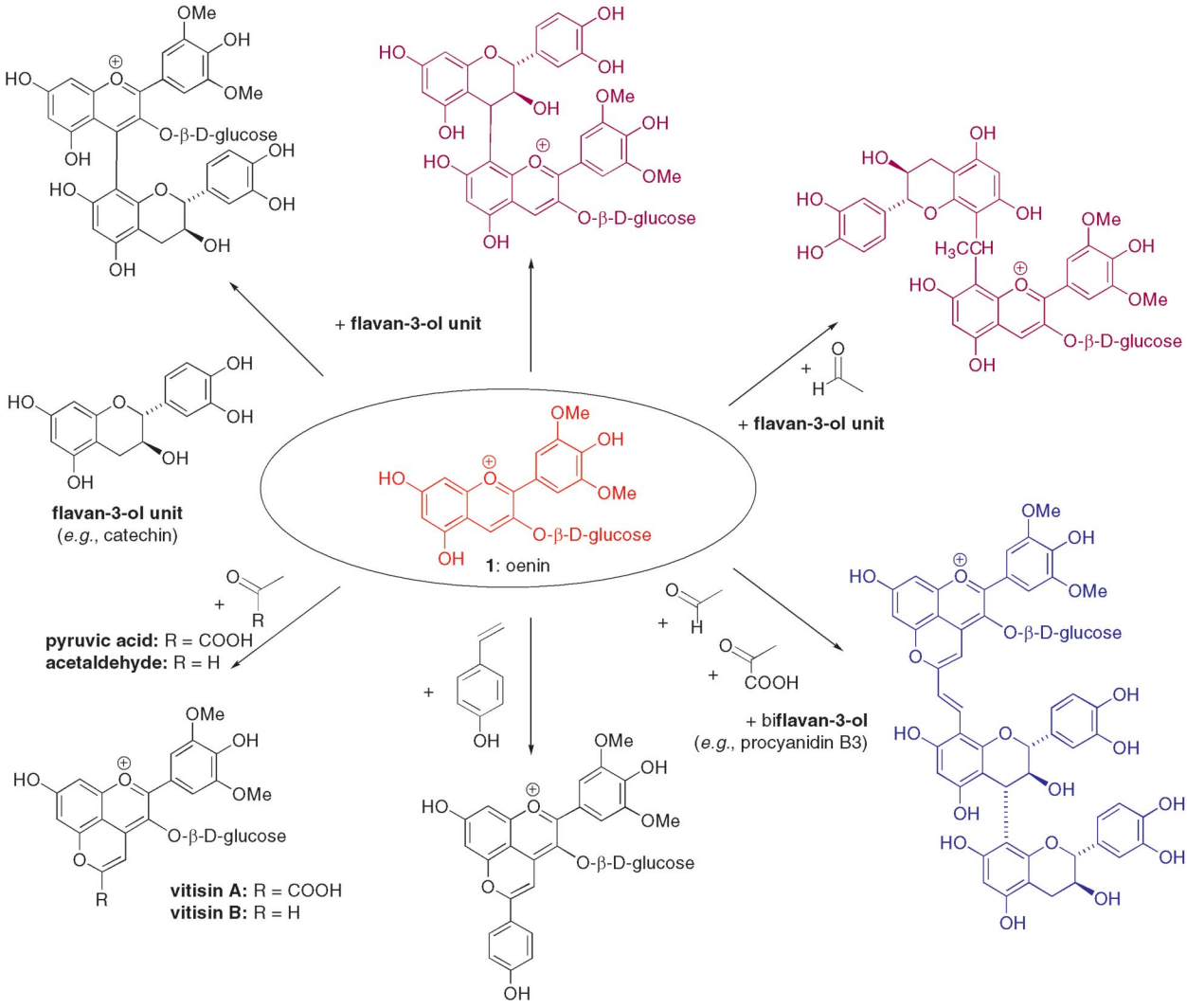

Scheme 1. From red grape oenin (**1**) to either bluer or more orangey wine genuine pigments.[2–7]

Results and Discussion

The condensation reaction between vescalagin (**3**), isolated from *Quercus robur* heartwood, and oenin (**1**) was performed in an acidic organic solution (i.e., 1.5% TFA/THF, v/v) and furnished the anthocyano-vescalagin **4**, as described previously (Scheme 2).[12a] The feasibility of this condensation reaction in wine had previously been confirmed by observing the formation of **4** in a standard wine model reaction mixture (i.e., 5 g/L of tartaric acid in 12% EtOH/H_2O, v/v, adjusted to pH 3.2; Figure 1).[12a]

The anthocyano-vescalagin **5** was prepared from **3** and commercially available malvidin (**2**) in a manner similar to that followed for **4**. Both of these compounds resulted from an acid-catalyzed nucleophilic substitution at the C-1 center of **3** with retention of the configuration (Scheme 2). Their regio- and stereochemistries were determined by NMR analyses: (i) the C-1 connectivity with the vescalagin unit was determined on the basis of the observation of strong HMBC correlations between its 1-H atom and some of the aromatic carbon atoms of the anthocyani(di)n unit A-ring, and the β-orientation of the anthocyani(di)n unit at C-1 was deduced from a Karplus interpretation of the small coupling constant (i.e., ^3J = 2.0 Hz) between the 1-H and 2-H protons of the glucose moiety of the vescalagin unit,[12] (ii) the question of whether the anthocyani(di)n unit is linked through either its C-6′ or C-8′ atom to the vescalagin unit was answered on the basis of our interpretation of diagnostic HMBC correlations exhibited by the flavylium A/C-ring fusion carbon atoms (i.e., C-4′a and C-8′a).[13] These carbon atoms were easily assigned on the basis of their characteristic chemical shifts and HSQC/HMBC correlations within the flavylium moiety (see Tables S1 and S2 in the Supporting Information). The strong HMBC correlation between C-4′a and either 6’-H or 8’-H combined with the lack of correlation between C-8′a and either 6’-H or 8’-H enabled the assignment of the correlating proton to 6’-H and not 8’-H. Furthermore, the observation of strong

 © 2010 Wiley-VCH Verlag GmbH & Co. KGaA, Weinheim

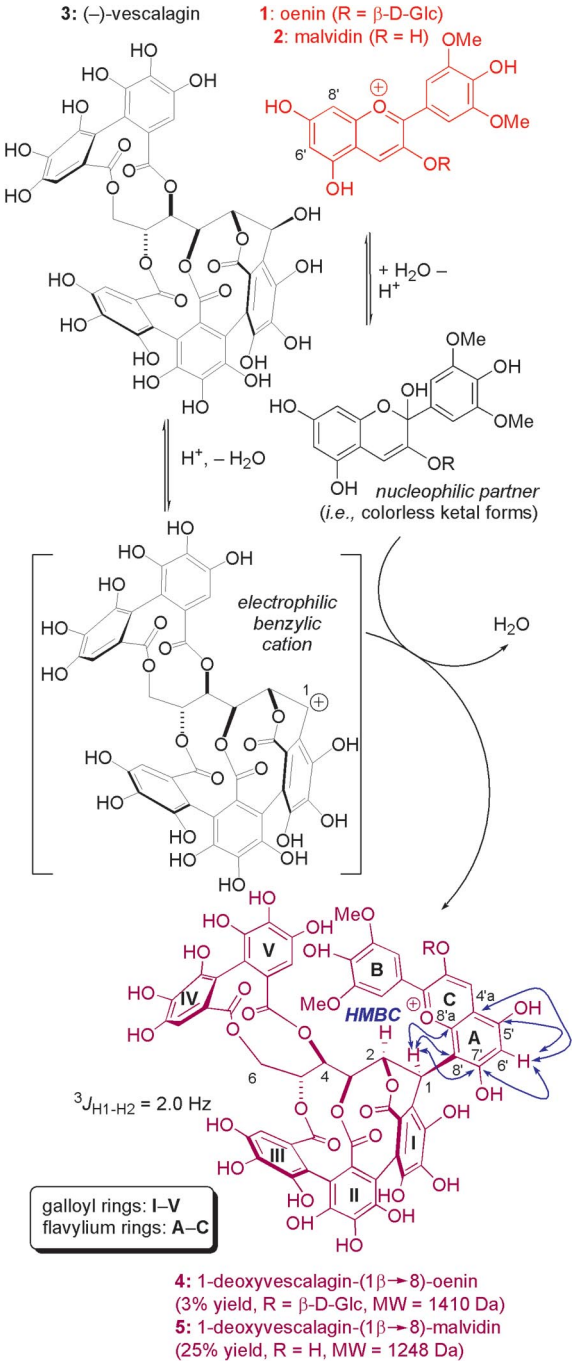

Scheme 2. Acid-catalyzed formation of the anthocyano-vescalagin condensation products **4** and **5** starting from vescalagin (**3**) and either oenin (**1**) or malvidin (**2**) in an acidic organic solution (i.e., 1.5% TFA/THF, v/v, 60 °C, 1–3 d).

two-bond HMBC correlations between this shielded proton and both C-5′ and C-7′ on the flavylium A-ring is in agreement with this assignment of 6'-H. We also performed a ROESY experiment which revealed through-space connectivities between B-ring protons (i.e., 2′′-H and 6′′-H) and the 1-H/2-H protons of the vescalagin moiety (Figure 2). Such connectivities are known to be characteristic of a C-8′ linkage of the anthocyani(di)n moiety, the observed spatial proximity between the B-ring protons and 1-H/2-H protons

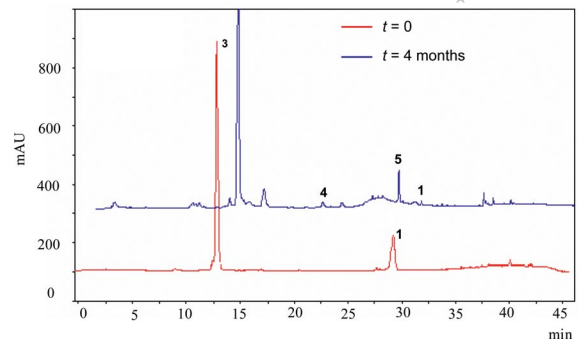

Figure 1. HPLC detection of the formation of adducts **4** and **5** starting from vescalagin (**3**) and oenin (**1**) in a wine model solution (i.e., 5 g/L of tartaric acid in 12% EtOH/H_2O, v/v, adjusted to pH 3.2, room temp.).[12a]

being structurally fulfilled only in the case of a C-8′ (and not a C-6′!) linkage.[4b,5] Hence, the C-8′/C-1 connectivity between the anthocyani(di)n and the vescalagin moieties of the anthocyano-ellagitannins **4**/**5** have here been unambiguously confirmed.

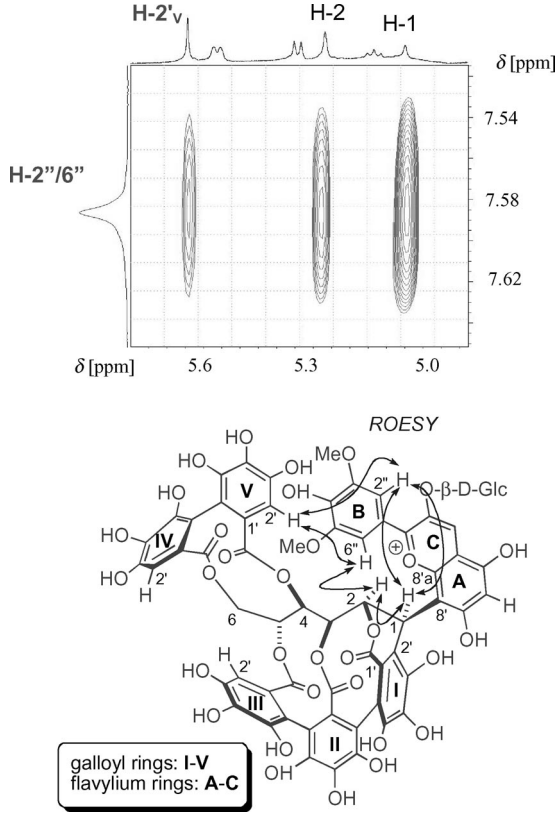

Figure 2. Diagnostic portion of the ROESY correlation map of 1-deoxyvescalagin-(1β→8)-oenin (**4**) recorded in 1% TFA/MeOD (v/v). For an estimation of through-space interatomic distances, see Table 4.

The most intriguing and wine-related aspect of the formation of these anthocyano-ellagitannins is their remarkable change in color compared with that of their precursors. Indeed, in the course of these hemisyntheses, the initial red reaction mixture gradually turned to deep purple, both in

 © 2010 Wiley-VCH Verlag GmbH & Co. KGaA, Weinheim

the 1.5% TFA/THF medium and in the wine model solution at pH 3.2 (Figure 1). It is important to recall that, in mildly acidic aqueous solutions, anthocyanins, such as oenin (**1**), typically undergo reversible transformations leading to mixtures of colored and colorless species.[14] Thus, the addition of water to the colored flavylium ion $\mathbf{AH^+}$ yields a colorless hemiketal **B** that is in fast cycle–chain equilibrium with the (*E*)-chalcone $\mathbf{C_E}$, itself in slow equilibrium with the (*Z*)-chalcone $\mathbf{C_Z}$ (Scheme 3).

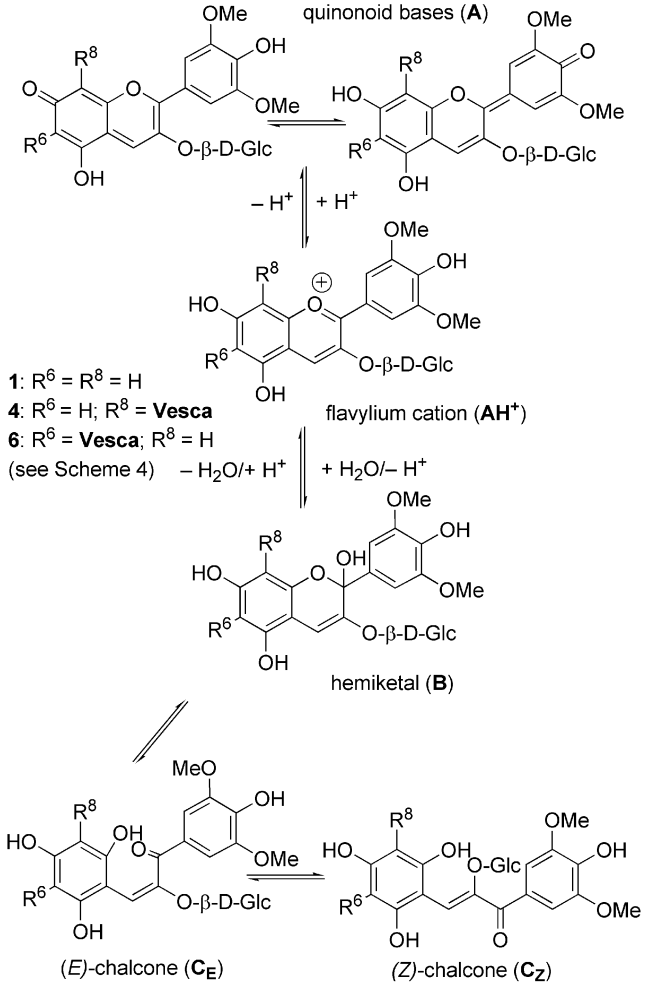

Scheme 3. Structural transformations of anthocyanins **1** and **4** in mildly acidic aqueous solutions [**Vesca** = vescalagin (**3**)-derived moiety].

Alternatively, proton transfer from $\mathbf{AH^+}$ yields colored tautomeric quinonoid bases **A**. One can assume with confidence that our novel pigment 1-deoxyvescalagin-(1β→8)-oenin (**4**) behaves similarly. In this context, rotation around the C-4′–C-4′a bond of the (*E*)-chalcone $\mathbf{C_E}$ followed by C-ring reclosure and dehydration is a conceivable process that could cause the regioisomerization of **4** to the less sterically hindered 1-deoxyvescalagin-(1β→6)-oenin (**6**), however, this C-6 regioisomer was not isolated (Scheme 4).

We then examined whether any modulation of such a pH-dependent equilibrium could be brought about by the presence of the vescalagin unit with a view to perhaps finding an explanation for the change of color. From the pH dependence of the apparent rate constant of hydration and of the visible absorbance at the end of the hydration process (i.e., before $\mathbf{C_Z}$ formation) and after complete equilibration, the following kinetic and thermodynamic parameters can be determined:[15]

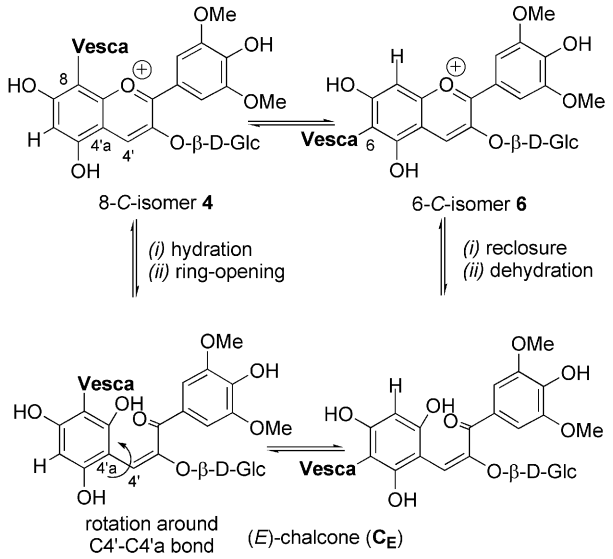

Scheme 4. Putative regioisomerization process of 1-deoxyvescalagin-(1β→8)-oenin (**4**) to 1-deoxyvescalagin-(1β→6)-oenin (**6**) in mildly acidic aqueous solutions [**Vesca** = vescalagin (**3**)-derived moiety].

$$K_h = \frac{k_h}{k_{-h}} = 10^{-pH}\frac{(B)+(C_E)}{(AH^+)} \qquad K_a = 10^{-pH}\frac{(A)}{(AH^+)}$$

$$K_t = \frac{(C_Z)}{(B)+(C_E)}$$

Their values are summarized in Table 1 for pigment **4** and its precursor **1**. A comparative interpretation of these data shows that the vescalagin moiety does not alter the acidic properties of the flavylium cation because the pK_a value is essentially unaltered. However, it appears that **4** is less prone than its precursor (lower pK_h) to forming a colorless hemiketal. With respect to hydration, **4** can thus be claimed to be a more stable pigment than **1**. This enhanced stability is in fact due to a faster dehydration of the hemiketal **B** derived from **4** (see k_{-h} values in Table 1). Although the pK_h difference is rather weak, it is worth noting that its impact on the percentage of colored species at wine pH (e.g., 3.2) is significant (i.e., 50% for **4** vs. 30% for **1**).

Table 1. Kinetic and thermodynamic parameters for the structural transformation of the selected anthocyanins (0.1 M citrate/phosphate buffer, ionic strength set at 1 M by NaCl, T = 25 °C).[a]

Anthocyanin	pK_h	pK_a	k_h / s^{-1}	k_{-h} / $M^{-1}s^{-1}$	K_t
Oenin (**1**)[16]	2.83	3.78	5.5×10^{-2}	37	–
Oenin-8-*C*-vescalagin (**4**)	3.19	3.87	6.8×10^{-2}	104	0.1

[a] For details of the calculations, see the Supporting Information.

 © 2010 Wiley-VCH Verlag GmbH & Co. KGaA, Weinheim

The visible spectra of **1** and **4**, as well as their corresponding aglycones **2** and **5**, were first recorded at pH 1 (i.e., in the pure flavylium form). The visible absorption band of both **4** and **5** showed a bathochromic shift of about 25 nm with respect to **1** and **2**, thus corroborating the purple hue observed for **4** and **5** (Figure 3, Table 2). The same observation was made at wine pH.

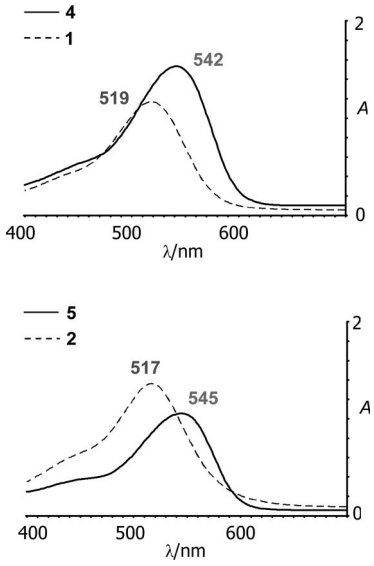

Figure 3. Visible spectra of oenin (**1**), malvidin (**2**) and the anthocyano-ellagitannins **4** and **5** in aqueous 1 M HCl solutions (pH 1). Estimated molar absorption coefficients (ε [L/mol·cm], 1 cm optical pathlength): **1**: ε = 26000, $c = 4.8 \times 10^{-5}$ mol/L; **2**: ε = 18400, $c = 6.7 \times 10^{-5}$ mol/L; **4**: ε = 16300, $c = 9.4 \times 10^{-5}$ mol/L; **5**: ε = 15700, $c = 7 \times 10^{-5}$ mol/L.

Table 2. Maximum absorbance wavelengths for oenin (**1**), malvidin (**2**), 1-deoxyvescalagin-(1β→8)-oenin (**4**), and 1-deoxyvescalagin-(1β→8)-malvidin (**5**) in four different acidic solutions.[a]

Solution	pH	λ_{max} (**1**)	λ_{max} (**4**)	Bathochromic shift
A	1	519 nm	542 nm	23 nm
B	1	518 nm	541 nm	23 nm
C	3.2	524 nm	544 nm	20 nm
D	3.2	529 nm	545 nm	16 nm
Solution	pH	λ_{max} (**2**)	λ_{max} (**5**)	Bathochromic shift
A	1	517 nm	545 nm	28 nm
B	1	518 nm	541 nm	23 nm
C	3.2	521 nm	546 nm	25 nm
D	3.2	523 nm	n.d.	n.d.

[a] **A**: Aqueous 1 M HCl solution adjusted to pH 1 by the addition of 1 M NaOH (see Figure 3). **B**: Aqueous 0.02 M HCl and 0.2 M KOH buffer solution (pH 1). **C**: Wine model solution composed of 12% EtOH/H_2O (v/v) and tartaric acid (5 g/L) adjusted to pH 3.2 by the addition of 1 M NaOH. **D**: Aqueous 0.1 M HCl and 0.1 M potassium hydrogen phthalate buffer solution (pH 3.2). n.d.: not determined.

A bathochromic shift is often observed when anthocyanins are involved in copigmentation with colorless phenolic compounds.[1] The bathochromism observed here could therefore simply be due to intermolecular interactions between the anthocyanidin chromophore of one molecule of **4** (or **5**) and the galloyl-derived unit of the vescalagin moiety of another. However, such a self-association process does not seem to be responsible for the modulation of color because dilution of a solution of **4** (pH 1) from 1.2×10^{-4} to 6.9×10^{-6} mol/L had no effect on its λ_{max} value (Figure 4).

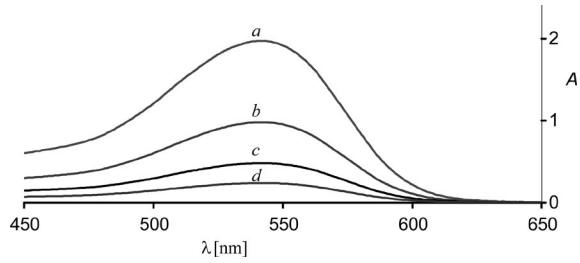

Figure 4. Visible spectra of 1-deoxyvescalagin-(1β→8)-oenin (**4**) at different concentrations in aqueous 1 M HCl (pH 1). a) 1.2×10^{-4} mol/L; b) 6.0×10^{-5} mol/L; c) 3.1×10^{-5} mol/L; d) 6.9×10^{-6} mol/L (1 cm optical pathlength).

Furthermore, we evaluated the intermolecular copigmentation ability of vescalagin (**3**) towards oenin (**1**) at pH 1 and 3.2 (Figure 5). Based on the fact that the flavylium form of **1** far from confering much color to a solution in the pH range of about 3 to neutrality (see Table 1), vescalagin (**3**) could indeed act as a copigment of **1** because the addition of **3** clearly enhances the color of the solution when [copigment]/[pigment] > 5 (Figure 5, b). However, as can be seen in Figure 5, no significant bathochromic shift was observed, thus confirming that the purple hue of the anthocyano-vescalagin adduct **4** (and **5**) is not a result of intermolecular interactions between the vescalagin and the flavylium units of different molecules of **4** (or **5**).

Having thus ruled out the possibility of intermolecular copigmentation, we turned our attention to similar but intramolecular interactions. The geometrical and electronic spectral criteria of our anthocyano-ellagitannins were first examined by computational means (see the Supporting Information for details). Because the observed bathochromic shift appeared to be quasi-independent of the presence of the 3-*O*-glucosyl unit on the anthocyanidin chromophore (Figure 3), calculations were performed only on the aglycones malvidin (**2**) and 1-deoxyvescalagin-(1β→8)-malvidin (**5**). Geometry optimizations were carried out by using AM1 parameters[17] with H_2O as the solvent. UV/Vis spectra were then calculated from the resulting minimum-energy conformations using the ZINDO method. To check the reliability of this semi-empirical approach, the ZINDO-calculated spectrum of **2** was compared with that obtained by using time-dependent density functional theory (TD-DFT) at the B3LYP/6-31G(d) level of theory. Both calculations correctly predicted the experimental λ_{max} value of 517 nm for **2** [i.e., 516 and 520 nm by ZINDO and B3LYP/6-31G(d), respectively]. However, the first-allowed electronic transition (i.e., single excitation mainly from HOMO to LUMO) calculated for **5** using the ZINDO method also gave a value of 517 nm (see the Supporting Information for details on these calculations). This failure to predict the bathochromism of the visible band of **5** led us to evaluate the

 © 2010 Wiley-VCH Verlag GmbH & Co. KGaA, Weinheim

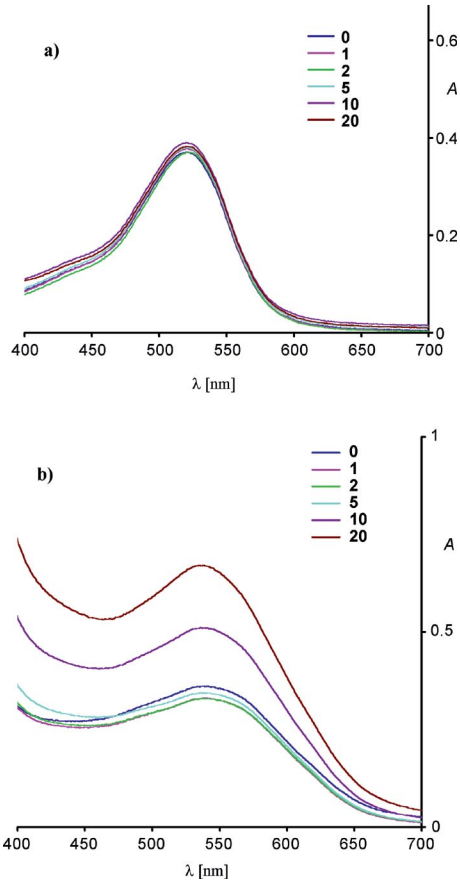

Figure 5. a) Visible spectra of oenin (**1**; 2.5×10^{-5} M) and vescalagin (**3**) at 0, 1, 2, 5, 10, and 20 [copigment]/[pigment] molar ratios (pH = 1.0, T = 25 °C, optical pathlength = 1 cm, solvent = aqueous HCl/KCl buffer, ionic strength = 0.40 M). b) Visible spectra of oenin (**1**; 3.8×10^{-4} M) and vescalagin (**3**) at 0, 1, 2, 5, 10, and 20 [copigment]/[pigment] molar ratios (pH = 3.2, T = 25 °C, optical pathlength = 1 cm; solvent = aqueous KH_2PO_4 buffer, ionic strength = 0.20 M).

ZINDO procedure by modifying the size of its active space, which involves every single excitation from a set of n occupied molecular orbitals (MOs) to a set of m unoccupied MOs (the $m + n$ MO defines the active space).

Calculations were initially performed by arbitrarily setting n and m at 80. Examination of the dependence of the size of this active space ($n = m$) on calculated spectra revealed that the first-allowed transition for **2** reaches an asymptotic value of 517 nm for $n \geq 60$, whereas the value of λ for the hybrid **5** appears to follow a slow but steady progression towards bathochromically shifted values for $n > 110$ (Figure 6). Unfortunately, we could not calculate any value of λ for $n > 110$ because the ZINDO procedure does not permit the size of the active space to be extended (see the Supporting Information).

Notwithstanding such a failure to predict the bathochromism of the visible band of **5**, we examined the effect of solvent by recording the visible spectra of **4** in H_2O, CH_3CN, MeOH, and THF (2.4×10^{-5} mol/L). A trend towards an increase in λ_{max} with decreasing solvent polarity was observed (Figure 7 and Table 3). Such a negative solvatochromism seems to be a general property of anthocyanins that has been interpreted in terms of the low-energy excited state of the flavylium nucleus being less polar than the ground state.[18]

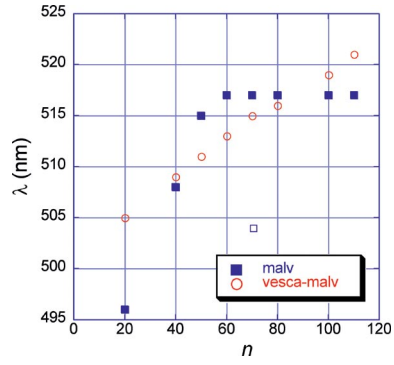

Figure 6. Evolution of the ZINDO-calculated first-allowed transition for malvidin (**2**, malv) and 1-deoxyvescalagin-(1β→8)-malvidin (**5**, vesca-malv) as a function of the size of the active space ($n = m$).

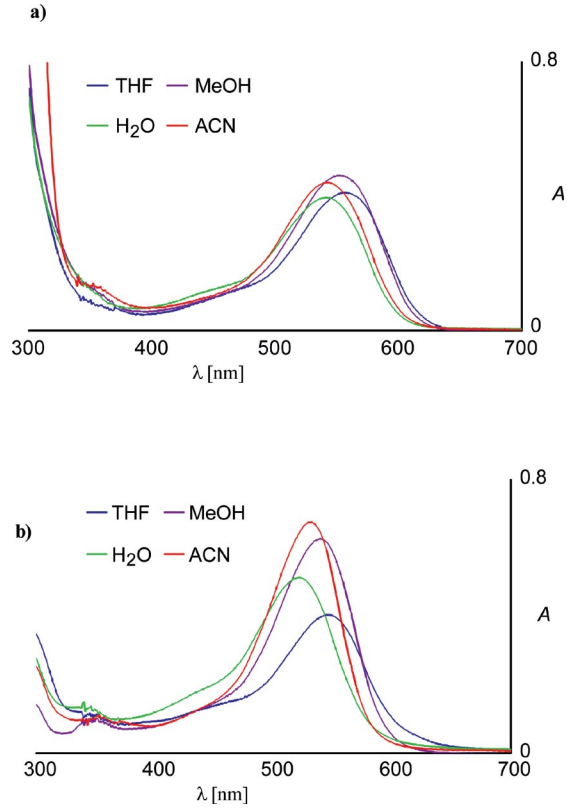

Figure 7. Evaluation of solvent effects on a) the visible spectra of 1-deoxyvescalagin-(1β→8)-oenin (**4**; 2.4×10^{-5} M) in four different solvents containing 1% TFA (v/v) (T = 25 °C, optical pathlength = 1 cm) and b) the visible spectra of oenin (**1**; 2.0×10^{-5} M) in four different solvents containing 1% TFA (v/v) (T = 25 °C, optical pathlength = 1 cm).

It has been claimed that such a change in electronic distribution in the flavylium nucleus could strengthen its aptitude for stacking phenolic rings, thereby providing a conceivable rationale for the bathochromic effect typically ob-

 © 2010 Wiley-VCH Verlag GmbH & Co. KGaA, Weinheim

Table 3. Maximum absorbance wavelengths and molar absorption coefficients for oenin (**1**) and 1-deoxyvescalagin-(1β→8)-oenin (**4**) in four different solvents containing 1% TFA (v/v). Pigment concentrations: [**1**] = 2.0×10^{-5} M and [**4**] = 2.4×10^{-5} M (T = 25 °C, optical pathlength = 1 cm).

	Oenin (**1**)		Pigment (**4**)			
	λ_{max} (nm)	$\varepsilon_{\lambda max}$[a]	λ_{max} (nm)	$\varepsilon_{\lambda max}$[a]	$\Delta\lambda_{max}$ (nm)	$\Delta\varepsilon_{\lambda max}$[a]
H_2O	522	24.5	541	16.5	19	8.0
CH_3CN	532	32.2	541	18.4	9	13.8
MeOH	539	29.9	552	19.3	13	10.6
THF	547	19.3	557	17.1	10	2.2

[a] Expressed in 10^3 L/mol·cm.

served upon copigmentation.[18] To corroborate the plausibility of such a claim in the case of pigments **4** and **5**, we had to find evidence of an intramolecular interaction involving their flavylium units. A closer look at the ^{1}H NMR spectroscopic data of **4** and **5** indicates an abnormally upfield chemical shift for the 2′-H of the galloyl-derived V-ring (i.e., 5.65 and 5.68 ppm), whereas the 2′-H atoms of the III- and IV-rings resonate in the range 6.50–6.80 ppm (see Figure 2 and Tables S1 and S2 in the Supporting Information). Such a large upfield shift (ca. 1 ppm) of 2′$_V$-H in **4** and **5** suggests that this proton is under the influence of an anisotropic effect putatively emanating from an interaction with the flavylium moiety, as previously observed, inter alia, in the intramolecular face-to-face stacking conformation of the dicaffeoylated anthocyanin gentiodelphin.[19] Here, the possibility of such a stacking was confirmed by the observation on the ROESY correlation map of **4** of through-space connectivities between 2′$_V$-H and the 2′′-H and 6′′-H atoms of the flavylium B-ring (see Figure 2). Calibration of this data map revealed a mean distance between these protons of 3.0 ± 0.4 Å (Table 4), which is less than the equilibrium van der Waals' separation of 3.4 Å. Taken together, these NMR spectroscopic data demonstrate that the galloyl-derived V-ring and the flavylium B-ring of **4** experience intramolecular contacts, possibly by van der Waals or charge-transfer interactions.[19] These interactions seem largely to be retained in the transition state of the hydration process because the corresponding rate constant is very close to that of oenin (**1**), but they are probably much weaker or absent in the hemiketal **B** such that the activation energy barrier for dehydration is lower for **4** (higher k_{-h}, see Table 1 and Schemes 3 and 4).

Conclusions

The bathochromism of the visible band of the anthocyano-ellagitannin **4** (and **5**) relative to that of the corresponding free anthocyani(di)n component **1** (or **2**) can arise either from stronger intramolecular interactions between their flavylium and vescalagin 4,6-HHDP moieties in the low-energy excited state of the flavylium ion[18] or from a charge-transfer contribution.[21] Although the exact cause of this bathochromism is still hypothetical at the fundamental level, the results described herein constitute a first plausible molecular-level explanation of the red-to-purple color evolution observed during the early stages of wine-maturing processes in oak barrels (or with the addition of oak chips), and possibly involving oak ellagitannins.

Experimental Section

General: Oenin (**1**) was obtained by extraction from Merlot grapes and purification by centrifugal partition chromatography[22] (see the Supporting Information for details). Malvidin (**2**) was purchased from Extrasynthese as its chloride salt. (–)-Vescalagin (**3**) was extracted from *Quercus robur* heartwood and purified as described previously.[17,23] The Amberlist XAD-7 HP resin was purchased from Supelco. Tetrahydrofuran (THF) was purified by distillation from sodium/benzophenone under N_2 immediately before use. Methanol (MeOH), acetonitrile (CH_3CN), ethyl acetate (EtOAc), and *n*-butanol (BuOH) were of HPLC quality and Milli-Q (Millipore) water was used for HPLC analyses and purifications. The different mobile phases used for all HPLC analyses and separations were composed of solvent A [H_2O/H_3PO_4 (999:1)] and solvent B [MeOH/H_3PO_4 (999:1)], or solvent C [H_2O/HCOOH (990:10)] and solvent D [MeOH/HCOOH (990:10)], or solvent E [H_2O/HCOOH (950:50)] and solvent F [MeOH/HCOOH (950:50)], or solvent G [H_2O/HCOOH (996:4)] and solvent H [MeOH/HCOOH (996:4)] (see the Supporting Information for details of the HPLC equipment used). IR spectra were recorded with a FT-IR Perkin–Elmer Paragon 1000 PC spectrometer. Low- and high-resolution liquid secondary ion mass spectra (LSIMS, HRMS) were obtained from the Centre d'Etudes Structurales et d'Analyses des Molécules Organiques (CESAMO), Université Bordeaux 1, and

Table 4. Interatomic distances between 2′′-H/6′′-H_B and 2′-H_V, and 1-H, and 2-H.[a,b]

	ROESY 298 K $V_{ij} \longrightarrow d_{ij}$		ROESY 283 K $V_{ij} \longrightarrow d_{ij}$		Average distance with H-2''/6''
H-1	0.181 → 2.4Å	0.48 → 2.1Å	0.36 → 2.7Å	0.089 → 2.7Å	2.3 ± 0.4 Å
H-2	0.042 → 3.1Å	0.015 → 3.7Å	0.16 → 2.5Å	0.171 → 2.5Å	2.9 ± 0.4 Å
H-2′$_V$	**0.025 → 3.4Å**	**0.047 → 2.6Å**	**0.12 → 2.6Å**	**0.054 → 3.0Å**	**3.0 ± 0.4 Å**

[a] See Figures 2 and S8 in the Supporting Information for details. [b] The intensity V_{ij} of a ROESY cross-peak is related to the inverse sixth power of the interatomic distance d_{ij} between two spins i and j (isolated spin pair approximation ISPA).[20] The cross-peaks in the spectra were integrated separately for each side of the diagonal and an average was taken with the different values. The cross-peak intensity that corresponds to the covalently fixed distance of 1.8 Å between the two geminal protons 6-H was used for internal calibration.

 © 2010 Wiley-VCH Verlag GmbH & Co. KGaA, Weinheim

from the Centre Régional de Mesures Physiques de l'Ouest (CRMPO), Université Rennes 1.

Hemisynthesis of 1-Deoxyvescalagin-(1β→8)-oenin (4)[12a]

In Organic Solution: Oenin chloride (**1**; 55 mg, 0.104 mmol) and (–)-vescalagin (**3**; 84 mg, 0.09 mmol) were dissolved in an anhydrous THF solution (10 mL) containing trifluoroacetic acid (150 μL). This reaction mixture was stirred at 60 °C for 3 d, after which time HPLC monitoring using a gradient elution (0–20 min: 0–20% solvent B; 20–35 min: 20–100% solvent B; 35–40 min: 100% solvent B) with a flow rate of 1.0 mL/min indicated no further formation of **4**. The reaction progress was also monitored by HPLC/ESIMS using a different gradient elution (0–20 min: 0–20% solvent D; 20–35 min: 20–100% solvent D; 35–40 min: 100% solvent D) with a flow rate of 1.0 mL/min. The mixture was then evaporated and the residue was dissolved in water (10 mL) and freeze-dried to furnish a reddish purple powder (144 mg). This powder was separated by semi-preparative HPLC using a gradient elution (0–20 min: 0–30% solvent F; 20–24 min: 30–100% solvent F; 24–36 min: 100% solvent F) with a flow rate of 16 mL/min^{-1} to furnish, after freeze-drying of the corresponding fractions, **1** (10 mg, 19%), **3** (60 mg, 71%), **4** (4 mg, 3%), and **5** (7 mg, 6%). This reaction was repeated four times to afford 14 mg of **4** as an amorphous deep-purple powder. IR (KBr): $\tilde{\nu}$ = 3410, 1742 cm^{-1}. ^{1}H NMR [400 MHz, [D$_4$]MeOH/TFA (99:1)], see Table S2 in the Supporting Information. ^{13}C NMR [100 MHz, [D$_4$]MeOH/TFA (99:1)], see Table S2 in the Supporting Information. LSIMS: *m*/*z* (%) = 1409 (100) [M$^+$], 1247 (52). HRMS (LSIMS): calcd. for $C_{64}H_{49}O_{37}$ 1409.1953; found 1409.1988.

In the Wine Model Solution: Oenin chloride (**1**; 1.1 mg, 0.002 mmol) and (–)-vescalagin (**3**, 2 mg, 2.1 μmol) were dissolved in a standard wine model solution (1.5 mL) composed of a 12% (v/v) aqueous EtOH solution containing 5 g/L tartaric acid and adjusted to pH 3.2 by addition of a 1 M aqueous NaOH solution. This mixture was stirred at room temperature and kept in the dark for 4 months. The reaction progress was monitored by HPLC using a gradient elution (0–20 min: 0–20% solvent B; 20–35 min: 20–100% solvent B; 35–40 min: 100% solvent B) with a flow rate of 1.0 mL/min and indicated the formation of **4** and **5** (see Figure 1).

Hemisynthesis of 1-Deoxyvescalagin-(1β→8)-malvidin (5)[12a]

In Organic Solution: Malvidin chloride (**2**; 16.5 mg, 0.045 mmol) and (–)-vescalagin (**3**; 42 mg, 0.045 mmol) were dissolved in an anhydrous THF solution (20 mL) containing trifluoroacetic acid (300 μL). The reaction mixture was stirred at 60 °C for 3 d, after which time HPLC monitoring using a gradient elution (0–20 min: 0–30% solvent B; 20–35 min: 30–100% solvent B; 35–40 min: 100% solvent B) with a flow rate of 1.0 mL/min indicated quasi-completion of the reaction. The reaction progress was also monitored by HPLC/ESIMS using a different gradient elution (0–20 min: 0–20% solvent H; 20–35 min: 20–100% solvent H; 35–40 min: 100% solvent H) with a flow rate of 1.0 mL/min. The mixture was evaporated and the residue was dissolved in water (30 mL) and freeze-dried to furnish a red powder (67 mg). This powder was separated by semi-preparative HPLC using a gradient elution (0–20 min: 0–10% solvent F; 20–35 min: 10–100% solvent F; 35–40 min: 100% solvent F) with a flow rate of 16 mL/min to furnish, after freeze-drying, pure **5** (14 mg, 25%) as an amorphous red powder. IR (KBr): $\tilde{\nu}$ = 3380, 1736 cm^{-1}. ^{1}H NMR [400 MHz, [D$_4$]MeOH/TFA (99:1)], see Table S1 in the Supporting Information. ^{13}C NMR [100 MHz, [D$_4$]MeOH/TFA (99:1)], see Table S1 in the Supporting Information. LSIMS: *m*/*z* (%) = 1270 (9) [MNa]$^+$, 1247 (40) [M]$^+$, 303 (11). HRMS (LSIMS): calcd. for $C_{58}H_{40}O_{32}$ 1248.1506; found 1248.1501.

Visible Absorbance Experiments: Visible absorption spectra were recorded with a Kontron Instrument-Uvikon 922 spectrophotometer or a Biotek Instrument-Uvikon XL spectrophotometer fitted with a plastic or quartz 10 mm cell width.

Molecular Modeling: The geometry of malvidin (**2**) was optimized by using the semi-empirical AM1 parametrization available in the AMPAC package[24,25] and by ab initio DFT with the three-parameter hydrid functional B3LYP and the 6-31G(d) basis set available in the Gaussian 03 package.[26] Similar molecular parameters were obtained by either calculation protocol. The main difference between the AM1 and DFT methods was the value of the dihedral angle between the phenolic B and the pyrylium C rings of the molecule, values of –16 or +3° were obtained by AM1 or DFT, respectively. The true minima were checked by vibrational calculations. The vescalagin unit of 1-deoxyvescalagin-(1β→8)-malvidin (**5**) was first fully minimized by a Monte-Carlo search using the MM3* force field.[17,27] As a result of the large number of atoms in this anthocyano-ellagitannin hybrid, further geometry optimization was only performed at the AM1 level. This was accomplished both in the gas phase and in water by using the SM5.2 protocol. The resulting geometries were qualitatively similar (see the Supporting Information for the Cartesian coordinates and details of the ZINDO calculations).

NMR Analysis: Spectra were recorded in the indicated solvent with a Bruker DPX 400NB NMR spectrometer equipped with a 5 mm direct QNP probe with gradient capabilities. Rotating frame nuclear Overhauser spectroscopy (ROESY) was performed at 283 and 298 K with 1024(t_2) × 256(t_1) data points in States-TPPI mode with presaturation of the water signal. A relaxation delay of 3 s and 32 scans per increment; a sweep width of 6000 Hz in two dimensions, and a ROESY spin-lock of 300 ms were applied. Data processing was performed with Topspin software using a sine-bell multiplication in two dimensions.

Supporting Information (see also the footnote on the first page of this article): Experimental and analytical procedures, molecular modeling details and full NMR spectroscopic data for compounds **4** and **5**.

Acknowledgments

The authors thank the Conseil Interprofessionnel du Vin de Bordeaux (Grant No. 8383/8384) and the Conseil Régional d'Aquitaine (Grant Nos. 20020306001F and 20000305002) for financial support.

[1] a) R. Brouillard, in: *The Flavonoids* (Ed.: J. B. Harborne), Chapman and Hall, London, **1988**, pp. 525–538; b) T. Goto, T. Kondo, *Angew. Chem. Int. Ed. Engl.* **1991**, *30*, 17–33; c) R. Boulton, *Am. J. Enol. Vitic.* **2001**, *52*, 67–87; d) K. Yoshida, M. Mori, T. Kondo, *Nat. Prod. Rep.* **2009**, *26*, 884–915.

[2] a) T. C. Somers, *Phytochemistry* **1971**, *10*, 2175–2186; b) H. Liao, Y. Cai, E. Haslam, *J. Sci. Food Agric.* **1992**, *59*, 299–305; c) R. Brouillard, S. Chassaing, A. Fougerousse, *Phytochemistry* **2003**, *64*, 1179–1186.

[3] a) J. C. Rivas-Gonzalo, C. Santos-Buelga, in: *Polyphenols, Wine and Health* (Eds.: C. Chèze, J. Vercauteren, R. Verpoorte), Kluwer, Dordrecht, **2001**, pp. 99–121; b) H. Fulcrand, V. Atanasova, E. Salas, V. Cheynier in *Red Wine Color: Revealing the Mysteries* (Eds.: A. L. Waterhouse, J. Kennedy), ACS, Washington, D.C., **2004**, pp. 68–88.

[4] For examples of oenin-(oligo)flavanol adducts, see: a) C. Dallas, J. M. Ricardo da Silva, O. Laureano, *J. Agric. Food Chem.* **1996**, *44*, 2402–2407; b) T. Escribano-Bailon, O.

 © 2010 Wiley-VCH Verlag GmbH & Co. KGaA, Weinheim

Dangles, R. Brouillard, *Phytochemistry* **1996**, *41*, 1583–1592; c) N. Mateus, A. M. S. Silva, C. Santos-Buelga, V. de Freitas, *J. Agric. Food Chem.* **2002**, *50*, 2110–2116; d) N. Mateus, A. M. S. Silva, J. C. Rivas-Gonzalo, C. Santos-Buelga, V. de Freitas, *J. Agric. Food Chem.* **2003**, *51*, 1919–1923; e) E. Salas, H. Fulcrand, E. Meudec, V. Cheynier, *J. Agric. Food Chem.* **2003**, *51*, 7951–7961; f) J. Pissara, S. Lourenço, A. M. Gonzalez-Paramas, N. Mateus, C. Santos-Buelga, V. de Freitas, *Anal. Chim. Acta* **2004**, *513*, 215–221; g) E. Salas, V. Atanasova, C. Poncet-Legrand, E. Meudec, J. P. Mazauric, V. Cheynier, *Anal. Chim. Acta* **2004**, *513*, 325–332.

[5] For examples of acetaldehyde-mediated couplings of oenin and other wine compounds, see ref.[4a–c]. See also: V. Atanasova, H. Fulcrand, C. Le Guenervé, V. Cheynier, M. Moutounet, *Tetrahedron Lett.* **2002**, *43*, 6151–6153.

[6] For examples of oenin-pyruvic acid adducts, see: a) J. Bakker, P. Bridle, T. Honda, H. Kuwano, N. Saito, N. Terahara, C. F. Timberlake, *Phytochemistry* **1997**, *44*, 1375–1382; b) J. Bakker, C. F. Timberlake, *J. Agric. Food Chem.* **1997**, *45*, 35–43; c) H. Fulcrand, C. Benabdeljalil, J. Rigaud, V. Cheynier, M. Moutounet, *Phytochemistry* **1998**, *47*, 1401–1407; d) N. Mateus, A. M. S. Silva, J. Vercauteren, V. de Freitas, *J. Agric. Food Chem.* **2001**, *49*, 4836–4840; e) A. M. Vivar-Quintana, C. Santos-Buelga, J. C. Rivas-Gonzalo, *Anal. Chim. Acta* **2002**, *458*, 147–155.

[7] For examples of oenin-vinylphenols adducts, see: a) H. Fulcrand, P.-J. Cameira dos Santos, P. Sarni-Manchado, V. Cheynier, J. Favre-Bonvin, *J. Chem. Soc. Perkin Trans. 1* **1996**, 735–739; b) M. Schwarz, T. C. Wabnitz, P. Winterhalter, *J. Agric. Food Chem.* **2003**, *51*, 3682–3687.

[8] P. Ribéreau-Gayon, P. Pontallier, Y. Glories, *J. Sci. Food Agric.* **1983**, *34*, 505–516.

[9] M. Del Álamo Sanza, I. Nevares Dominguez, S. García Merino, *Eur. Food Res. Technol.* **2004**, *219*, 124–132.

[10] M. Moutounet, P. Rabier, J. L. Puech, E. Verette, J.-M. Barillère, *Sci. Aliments* **1989**, *9*, 35–51.

[11] a) M. Mayer, H. Seitz, J. C. Jochims, K. Schauerte, G. Schilling, *Justus Liebigs Ann. Chem.* **1971**, 60–68; b) G.-I. Nonaka, T. Sakai, T. Tanaka, K. Mihashi, I. Nishioka, *Chem. Pharm. Bull.* **1990**, *38*, 2151–2156.

[12] a) S. Quideau, M. Jourdes, D. Lefeuvre, D. Montaudon, C. Saucier, Y. Glories, P. Pardon, P. Pourquier, *Chem. Eur. J.* **2005**, *11*, 6503–6513; b) S. Quideau, M. Jourdes, C. Saucier, Y. Glories, P. Pardon, C. Baudry, *Angew. Chem. Int. Ed.* **2003**, *42*, 6012–6014.

[13] For an example highlighting the privileged C-8′ nucleophilicity of oenin (**1**) and malvidin (**2**), see: S. Remy, H. Fulcrand, B. Labarbe, V. Cheynier, M. Moutounet, *J. Sci. Food Agric.* **2000**, *80*, 745–751.

[14] R. Brouillard, B. Delaporte, *J. Am. Chem. Soc.* **1977**, *99*, 8461–8468, and references therein.

[15] O. Dangles, N. Saito, R. Brouillard, *J. Am. Chem. Soc.* **1993**, *115*, 3125–3132.

[16] M. Duenas, E. Salas, V. Cheynier, O. Dangles, H. Fulcrand, *J. Agric. Food Chem.* **2006**, *54*, 189–196.

[17] The vescalagin unit of **5** was first fully minimized through a Monte-Carlo search using the MM3* force field, see: S. Quideau, T. Varadinova, D. Karagiozova, M. Jourdes, P. Pardon, C. Baudry, P. Genova, T. Diakov, R. Petrova, *Chem. Biodiversity* **2004**, *1*, 247–258.

[18] B. Alluis, N. Pérol, H. El Hajji, O. Dangles, *Helv. Chim. Acta* **2000**, *83*, 428–443.

[19] K. Yoshida, T. Kondo, T. Goto, *Tetrahedron* **1992**, *48*, 4313–4326.

[20] D. Neuhaus, M. P. Williamson, *The Nuclear Overhauser Effect in Structural and Conformational Analysis*, VCH Publishers, New York, **1989**.

[21] P. Ferreira da Silva, J. C. Lima, A. A. Freitas, K. Shimizu, A. L. Maçanita, F. H. Quina, *J. Phys. Chem. A* **2005**, *109*, 7329–7338.

[22] A. Foucault, L. Chevolot, *J. Chromatogr. A* **1998**, *808*, 3–22.

[23] A. Scalbert, L. Duval, S. Peng, B. Monties, C. Du Penhoat, *J. Chromatogr.* **1990**, *502*, 107–119.

[24] J. J. P. Stewart, *J. Mol. Mod.* **2004**, *10*, 155–164.

[25] AMPAC 8.0, Semichem, Inc., Shawnee, KS, © **1992**–**2004**.

[26] M. J. Frisch, G. W. Trucks, H. B. Schlegel, G. E. Scuseria, M. A. Robb, J. R. Cheeseman, J. A. J. Montgomery, T. Vreven, K. N. Kudin, J. C. Burant, J. M. Millam, S. S. Iyengar, J. Tomasi, V. Barone, B. Mennuci, M. Cossi, G. Scalmani, N. Rega, G. A. Petersson, H. Nakatsuji, M. Hada, M. Ehara, K. Toyota, R. Fukuda, J. Hasegawa, M. Ishida, T. Nakajima, Y. Honda, O. Kitao, H. Nakai, M. Klene, X. Li, J. E. Knox, H. P. Hratchian, J. B. Cross, C. Bakken, C. Adamo, J. Jaramillo, R. Gomperts, R. E. Stratmann, O. Yazyev, A. J. Austin, R. Cammi, C. Pomelli, J. W. Ochterski, P. Y. Ayala, K. Morokuma, G. A. Voth, P. Salvador, J. J. Dannenberg, V. G. Zakrzewski, S. Dapprich, A. D. Daniels, M. C. Strain, O. Farkas, D. K. Malick, A. D. Rabuck, K. Raghavachari, J. B. Foresman, J. V. Ortiz, Q. Cui, A. G. Baboul, S. Clifford, J. Cioslowski, B. B. Stefanov, G. Liu, A. Liashenko, P. Piskorz, I. Komaromi, R. L. Martin, D. J. Fox, T. Keith, M. A. Al-Laham, C. Y. Peng, A. Nanayakkara, M. Challacombe, P. M. W. Gill, B. Johnson, W. Chen, M. W. Wong, C. Gonzalez, J. A. Pople, *Gaussian 03 (Revison C.02)*, Gaussian, Inc., Wallingford, CT, **2004**.

[27] F. Mohamadi, N. G. J. Richards, W. C. Guida, R. Liskamp, M. Lipton, C. Caufield, G. Chang, T. Hendrickson, W. C. Still, *J. Comput. Chem.* **1990**, *11*, 440–467.

Received: October 6, 2009
Published Online: November 20, 2009

 © 2010 Wiley-VCH Verlag GmbH & Co. KGaA, Weinheim